AIAA JOURNAL
Vol. 47, No. 4, April 2009

Bayesian Wavelet Methodology for Damage Detection of Thermal Protection System Panels

Xiaomo Jiang*
General Electric Company, Greenville, South Carolina 29615
and
Sankaran Mahadevan† and Robert Guratzsch‡
Vanderbilt University, Nashville, Tennessee 37235

DOI: 10.2514/1.38503

This paper presents an intelligent computational methodology for loose-bolt detection in thermal protection panels, considering uncertainties in sensed data. The proposed methodology is based on the integration of a dynamic artificial neural network, wavelet signal analysis, and Bayesian probabilistic assessment. A dynamic fuzzy wavelet neural-network model is employed to perform the multiple-input/multiple-output nonparametric system identification of the panel using time-series data obtained from the panel under a healthy condition. The trained model is used to predict dynamic responses of the structural system under unknown conditions. Both predicted and sensed-time-history data are decomposed into multiple time–frequency resolutions using a discrete wavelet-packet transform method. The wavelet-packet component energy is computed in terms of the decomposed coefficients and used as a signal feature to detect loose bolts. The effectiveness of the selected features is assessed using both cross-correlation and cross-coherence metrics. The multivariate comparison in damage detection is handled by an interval-based Bayesian hypothesis-testing approach. The methodology is implemented to detect one loose bolt of a prototype thermal protection system panel with four mechanically bolted joints using experimental data collected at the U.S. Air Force Research Laboratory from seven different sensor configurations.

I. Introduction

A THERMAL protection system (TPS) plays a critical role in the structural safety and integrity of space operation vehicles (SOV). The TPS provides an SOV with the first line of defense against both the extreme-high-temperature environments during reentry and the severe mechanical loadings such as aerodynamic or acoustic pressure and debris impacts. Generally, the fuselage of an SOV is covered with TPS panels, which are attached to the vehicle's surface via mechanically bolted joints. Thus, the bolted joint becomes a critical mechanical component in the space structures. It not only provides structural load paths to other critical components in the SOV, but is also the path of energy dissipation and vibration damping in these components.

The bolted joints are subject to a variety of failure modes, such as self-loosening, shaking apart, stress cracking or fatigue, slippage, and separation [1]. If the fastening mechanism of any one panel in a TPS fails, the effectiveness of the TPS could become compromised, exposing the vehicle's entrails to the extreme environment, thereby compromising vehicle integrity and ultimately jeopardizing mission success and crew safety. Particularly, self-loosening is one of the most frequently observed failure modes for bolted joints. Undetected bolt-loosening causes hot air to enter the detachment gap at joints, which leads to subsystem malfunctions and, further, to the catastrophic loss of vehicle and crews. Therefore, a reliable and robust structural-health-monitoring (SHM) system is needed for detection of loose bolts in a TPS.

The development of an effective SHM system for loose-bolt detection depends on two important factors: sensing technology and an associated signal analysis and interpretation algorithm. Many sensor technologies (e.g., strain gauges, thermocouples, and accelerometers) are available for use in health monitoring and damage detection [2–5]. These traditional sensors are embedded in or attached to a structure at selected locations and used to measure the dynamic response of the structure with the purpose of monitoring the structural integrity and performance. Recently, many new sensor technologies have been developed for structural health monitoring, such as fiber-optic sensors [6], remote wireless or noncontact sensing technologies [7], and active and passive ultrasonic sensing methods [8]. In situ sensor systems have also been developed for high-temperature applications [9]. More recently, Blackshire et al. [10] and Blackshire and Cooney [11,12] developed and extensively applied surface-bonded piezoelectric transducers in experimental settings of aerospace materials. The piezoelectric transducer is also referred to as an *active sensor*, because it can both receive and generate signals and has high-performance characteristics, easy operability, long durability, and strong survivability under widely varying environmental conditions. This type of active sensor is therefore used in the laboratory experiments of this study.

After instrumentation of a structural system with sensors, an enormous amount of response data can be quickly collected. An efficient signal analysis and interpretation algorithm is then needed for effective damage detection. In general, the damage detection is realized by comparing the experimental measurements from the real TPS with the behavior of a calibrated or updated computational model, which is used as a reference for the healthy or undamaged condition. In the past decade, a number of researchers have proposed various techniques to detect the loosening of the TPS panel bolts [13–21]. These techniques can be divided into two categories: vibration-based and wave-propagation-based methods. The vibration-based technique detects the damage-induced changes to the dynamic response of the entire TPS under external excitations, in the context of both time and frequency domains. Features are usually extracted from the time-series measurement or modal analysis of the TPS panel. Time-series analysis-based pattern-recognition techniques, such as statistical classification [15] and autoregressive models with exogenous-input prediction [22–24], have been widely applied.

Received 11 May 2008; revision received 16 December 2008; accepted for publication 27 December 2008.

*Lead Engineer, General Electric Company, 300 Garlington Road, Mail Drop 256D. Member AIAA.
†Professor, Civil and Environmental Engineering, Station B 351831, 2301 Vanderbilt Place. Senior Member AIAA.
‡Graduate Student, Civil and Environmental Engineering, Station B 351831, 2301 Vanderbilt Place.

Recently, modal analysis-based techniques have been developed for detecting loose bolts [16] using the low-frequency mode shapes. Hundhausen et al. [25] derived the first few modal parameters of a bolted standoff TPS panel for nondestructive damage detection using the physics-based finite element analysis.

Recently, Peairs et al. [17] introduced an impedance-based method to detect the loose bolt in a TPS. This method requires the sensed data that was collected from the direct-contact region to the transducers and therefore may not be feasible for a hot TPS structure [20]. Yang and Chang [20,21] developed a wave-propagation-based bolt-loosening-detection technique by analyzing signal attenuation of sensors based on stress waves generated by an actuator. By comparing the signals generated from the same actuator at different times, an algorithm was developed to estimate the degree of bolt-loosening at a base bracket or at the top TPS panel. Clearly, the success of this kind of active SHM system depends not only on the diagnostic algorithms, but also on the design of the sensor/actuator network system in which the diagnostic signals are generated. Thus, the detectability of a loose bolt depends largely upon the location and configuration of the sensors and the actuators.

This paper pursues a new Bayesian wavelet-based diagnostic algorithm for detection of loose bolts in a TPS panel, targeted toward an active online SHM system. The proposed method employs a nonparametric system-identification approach and vibration test data. The bolt-loosening is assessed through comparing features extracted from measurements of the TPS under healthy and possibly damaged conditions (i.e., bolt-loosening).

Recently, the first author developed a dynamic fuzzy wavelet neural-network (WNN) model for multiple-input/single-output nonparametric identification of structures using the nonlinear autoregressive moving-average with exogenous (NARMAX) inputs [26]. In addition, an adaptive Levenberg–Marquardt least-squares (LM-LS) algorithm with a backtracking inexact linear search scheme was developed for training of the dynamic fuzzy WNN model [27]. In the nonphysically based approach, a system model is trained to approximate a physical structure under a healthy condition and to rapidly predict its response under various input excitations, thus reducing experimental expense by avoiding tests of a healthy structure under various excitations. Numerical results [26–32] have demonstrated that the fuzzy WNN model combined with an adaptive LM-LS algorithm provides an effective and efficient tool for approximation of structural dynamic responses. Therefore, the method is employed in this paper for the multiple-input/multiple-output system-identification part of the proposed detection methodology.

In the context of offline model validation and online damage detection based on time-series data, three important issues need to be addressed. First, what feature should be extracted from the signal for both validation and detection purposes? Usually, a time series consisting of thousands of data points contains rich information in the time domain. Useful information may be extracted to represent the signal pattern. The objectives of feature extraction are to reduce the dimensionality of the used data and to improve the efficiency and accuracy of online damage detection. Recently, Jiang and Mahadevan [33] developed a wavelet-packet component-energy-based method for multivariate model validation of dynamic systems. In this paper, the wavelet-packet component energy is used as the signal feature for damage detection.

The second issue is how to assess the effectiveness of selected features. Feature extraction will inevitably result in the loss of information from the original time series. The time-series data collected from a dynamic system typically contain useful information and also noise. Therefore, it is desirable to extract features that capture the characteristics of the dynamic system (information) and to separate those features that represent the disturbances (noise). Various approaches [34–40] have been proposed to assess the selected features. For example, Cho et al. [36] used the coherence spectra of the residuals in the frequency domain. Wu and Du [39] used various assessment criteria in both time and frequency domains. Yan and Gao [40] used a distance-measure-based assessment method. In this paper, both the *cross correlation* in time domain and the *cross coherence* in frequency domain between the original and reconstructed signals are used as the feature-selection rule.

The third issue to be considered is how to quantitatively assess the validity of the predictive model and how to timely evaluate the health status of TPS with respect to the bolted joints under uncertainty. In addition to the uncertainty in the analytical or predictive model, measurement data always contain uncertainty and noise resulting from the inspection setup and measurement conditions. Ignoring the uncertainties may result in erroneous decision-making. A Bayesian hypothesis-testing-based methodology is employed in this study as a quantitative measure to address the uncertainty in online loose-bolt detection.

In recent years, researchers [33,41–45] have developed Bayesian hypothesis-testing-based methods to validate computational mechanics models using measured data. These studies have demonstrated that the Bayesian approach is an effective tool for model validation under uncertainty. Both model validation and damage detection involve the comparison of two sets of data. Thus, the concepts and methods from model validation appear promising for transfer to real-time damage detection of bolted joints. To determine the most likely amount of damage, the Bayesian updating technique is applied to obtain the relative posterior probability of the damage hypothesis based on the difference of energy features extracted from the predicted and measured data.

Figure 1 shows the schematic diagram of loose-bolt detection using the active sensors, wavelet signal analysis, fuzzy WNN model, and Bayesian evaluation method. The detection system includes two stages: model development and loose-bolt detection. The model-

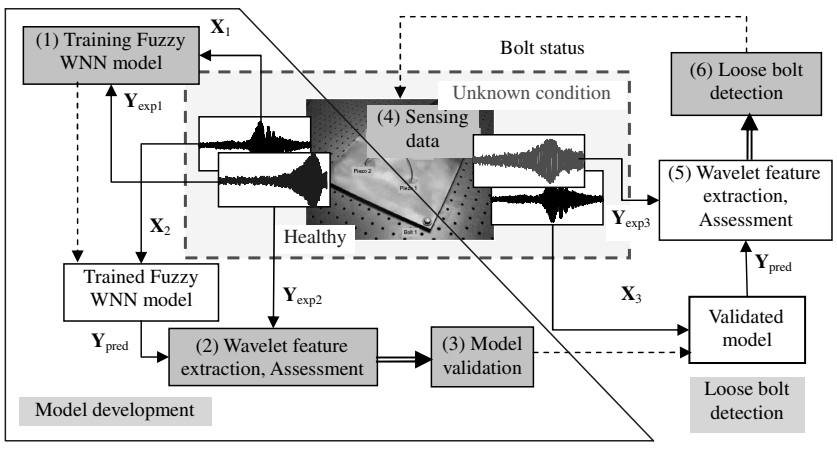

X = Excitation $\mathbf{Y}_{exp}$ = Experimental data $\mathbf{Y}_{pred}$ = Prediction output

Fig. 1 Online loose-bolt detection scheme using active sensing technology, wavelet signal analysis, fuzzy WNN model, and Bayesian evaluation method.

development stage contains three components (identified by boxes 1 to 3 in Fig. 1): 1) model construction and training using a set of data ($\mathbf{X}_1$ and $\mathbf{Y}_{\exp 1}$) collected from the TPS with a healthy condition, 2) feature extraction and assessment from a set of new data ($\mathbf{X}_2$ and $\mathbf{Y}_{\exp 2}$) with a healthy condition for model-validation purposes, and 3) model validation using the extracted features. The loose-bolt detection stage also contains three components (identified by the boxes 4 to 6 in Fig. 1): 4) a real-time data acquisition system to collect experimental data under unknown conditions ($\mathbf{X}_3$ and $\mathbf{Y}_{\exp 3}$), 5) feature extraction and assessment from the sensed data (similar to the second component in the first stage), and 6) loose-bolt detection using the extracted features. Note that the dashed-line arrow in Fig. 1 represents the information transmission (i.e., trained or validated model or bolt status), the single solid-line arrow represents the transmission of one data set (either predicted or sensed data), and the double-solid-line arrow represents the transmission of two data sets (features extracted from the predicted and sensed data). In the following sections, the five parts (the computational methods of the second and fifth components are the same) are presented in detail, and for illustration purposes, the proposed methodology is implemented to detect one loose bolt of a prototype TPS panel with four mechanically bolted joints using experimental data collected at the U.S. Air Force Research Laboratory from seven different sensor configurations.

II. Sensing Data

A. Prototype Description

The example problem discussed here provides a prototype SHM system to detect loose bolts in a simplified panel, described in detail by Olson et al. [46]. The panel shown in Fig. 2a was tested at the U.S. Air Force Research Laboratory. It consists of a heat-resistant 0.25-in.-thick aluminum panel of 12×12 in., held in place via four 0.25-in.-diam bolts, which are located 0.50 in. from the edges of the panel. The TPS panel or plate is considered to be healthy when all bolts are tightened to a nominal torque of 120 in. $\cdot$ lb. Different structural conditions are obtained by loosening one bolt at a time from the panel. A loose-bolt condition corresponding to 25% of the nominal bolt torque (30 in. $\cdot$ lb) represents damage. The analysis here is restricted to single-bolt damage and ignores simultaneous damage of multiple bolts. Thus, there are four damaged structural states, each corresponding to one of the four bolts being loose and one healthy structural state, in which all four bolts are tightened to 100% nominal torque. In this paper, the damaged structural state with bolt 1 loosening is used to illustrate the proposed detection methodology, because this is the most complicated case in the laboratory experiments (no sensor near bolt 1 to collect structural response data).

The surface-bonded piezoelectric transducer is used as the active sensor in the laboratory experiments of this study to generate and receive signals. Figure 2b shows a typical sensor layout, in which piezoelectric sensor location 1 (labeled as "Actuator") is fixed and this actuator is used to generate input excitations, and sensor locations S_2, S_3, and S_4 are variable and the three sensors are used to collect vibration response data at the three locations. Figure 2b also shows the locations of the 4 bolts, which hold the test structure in place.

B. Data Sensing of the Test Article

Seven sensor configurations were tested on the TPS test article shown in Fig. 2. The coordinates of sensors of the seven layouts are listed in Table 1 [47,48]. The coordinates (x, y) in Table 1 are with respect to the bottom left corner of the test article shown in Fig. 2b.

The SHM actuation signals (i.e., sine sweep from 0 to 1500 Hz) are generated and recorded using LabVIEW version 6.1 software and a National Instruments PXI 6052E data acquisition card. A fluke PM5193 programmable synthesizer/function generator produces a 1.5 V, peak-to-peak, swept-frequency sinusoid (0 to 1500 Hz in approximately 2.0 s) as the broadband excitation signal. The excitation function is amplified with a Krohn-Hite 7500 amplifier by a factor of 100 and applied to the test article via a 0.25-in.-diam piezoelectric disk transducer (i.e., a surface-bonded piezoelectric actuator, as discussed in Sec. II.A) at sensor location S_1 (labeled Actuator in Fig. 2). Structural responses are collected via piezoelectric sensors S_2, S_3, and S_4 at a frequency of 10 kHz and a 16-bit analog-to-digital conversion.

A total of 50 sets of test data were collected per sensor array configuration. It should be noted that the data recorded during experimental testing consists of time-series voltage signals captured by sensors S_2, S_3, and S_4. The signal applied via the actuator is also recorded as inputs to the damage-detection method developed in this study. The voltage time-series measurements are directly implemented in the damage detection. These experimental data are analyzed by using a Bayesian wavelet damage-detection approach developed below. As an illustrative example, Fig. 3 shows the sine-wave actuation excitation and the three response voltage signals of test article under a healthy condition for sensor configuration 2 in Table 1.

III. Dynamic Fuzzy Wavelet Neural-Network Emulator

The nonparametric dynamic fuzzy WNN model developed by Adeli and Jiang [26] is used in this research as a *neuroemulator* to predict the structural response in future time steps from the immediate past structural response and actuator excitation. The general dynamic input–output mapping in the model is

$$\hat{y}_i = \sum_{k=1}^{M} w_k \sum_{j=1}^{D} \varphi\left(\frac{X_{ij} - c_{kj}}{a_{kj}}\right) + \sum_{j}^{D} b_j X_{ij} + d, \quad i = 1, \ldots, N, \quad a \epsilon \Re, \quad \varphi(\cdot) \epsilon L^2(\Re) \tag{1}$$

where $\varphi(\cdot)$ is the nonorthogonal Mexican-hat wavelet function; X_{ij} is the jth value in the ith input vector X_i; c_{kj} is the jth value in the kth

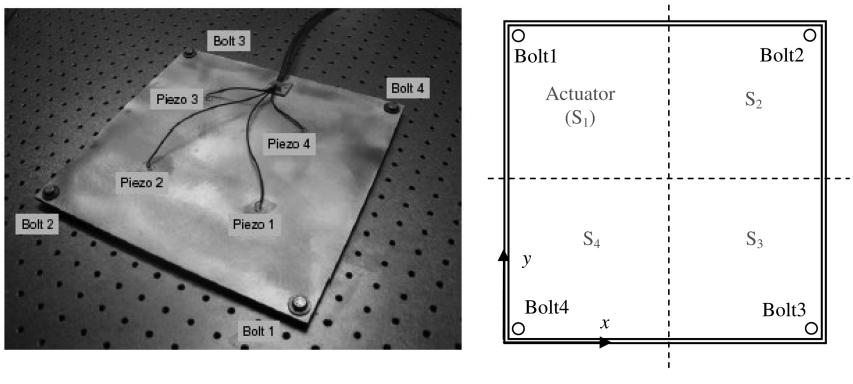

a) b)

Fig. 2 TPS test article: a) photograph (Olson et al. [46]) and b) schematic graph.

Table 1 Seven different sensor layouts

Sensor coordinates of sensor array	Coordinates of sensor		
	S_2	S_3	S_4
1	(8.5, 8.5)	(8.5, 3.5)	(3.5, 3.5)
2	(8.75, 6.75)	(6.0, 3.5)	(3.5, 0.75)
3	(7.0, 8.5)	(11.73, 0.27)	(5.75, 1.25)
4	(6.75, 8.75)	(9.25, 2.25)	(5.0, 5.0)
5	(11.0, 11.0)	(11.0, 1.0)	(1.0, 1.0)
6	(11.0, 7.0)	(6.5, 5.0)	(1.0, 5.0)
7	(7.0, 11.0)	(7.5, 1.0)	(1.75, 1.0)

cluster of the multidimensional input vector obtained using the fuzzy C mean clustering approach [49]; D is the input dimension or the size of the input vector in the NARMAX approach [50]; M is the number of wavelets, which is also equal to the number of the fuzzy clusters as well as the number of wavelet nodes used in the WNN model; $a_{kj} \neq 0$ denote the frequency (or scale) corresponding to the multidimensional input vector; W_k represents the kth wavelet coefficient linking the hidden node to the output; b_j is the weight of the link of the jth input to the output; d is a bias term, $\Re$ is the set of real numbers; and N is the number of input vectors.

Unlike conventional neural-network models such as a back-propagation neural network, the fuzzy WNN model is a dynamic neural network that preserves the time sequence of the input vectors and memorizes the past of the time-series data. The model is based on the integration of chaos theory (nonlinear dynamics theory), wavelets (a signal processing method), and two complementary soft-computing methods (i.e., fuzzy logic and neural networks). It has been demonstrated to provide more accurate nonlinear approximation than the conventional neural network [26].

Note that the fuzzy WNN model is trained using the data collected from the test article under a healthy condition (i.e., all bolts are 100% tightened) using the adaptive LM-LS algorithm [27,30]. Therefore, the trained model represents a structural system without any loose bolt, such that the predicted outputs should represent the structural responses without any damage. The trained model is then used to predict the dynamic responses of the test article under unknown conditions using the same test excitation and feedback model prediction. Refer to Adeli and Jiang [26] for details of training and testing of the fuzzy WNN model. Figure 4 shows the schematic diagram of a trained fuzzy WNN model for representing a TPS without any loose bolt. In the next section, wavelet-packet component-energy signatures will be extracted as signal features from both model predictions and real-time experimental measurements under the same excitation and then used to detect the loose bolt of the test article based on the Bayesian method described later.

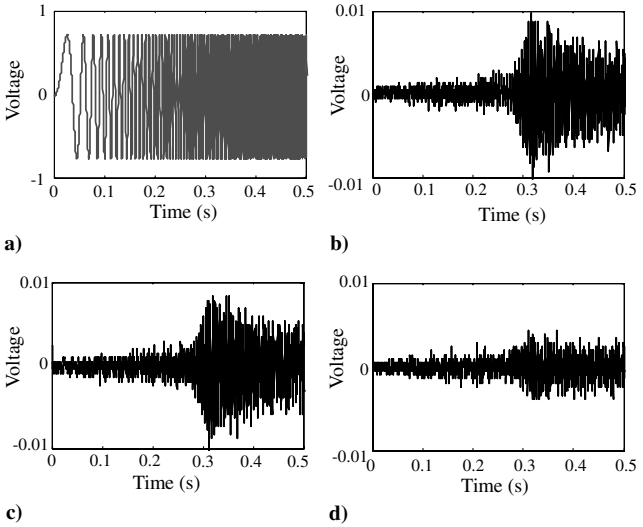

Fig. 3 Experimental data of test article under healthy condition from 0 to 0.5 s for sensor configuration 2 shown in Table 1: a) sine-wave excitation at actuator, b) response at S_2; c) response at S_3, and d) response at S_4.

IV. Wavelet Feature Extraction

A. Wavelet-Packet Component Energy

Wavelets consist of a family of mathematical functions used to represent a signal in both the time and frequency domains. A *wavelet transform* (WT) is a mathematical tool used to decompose a temporal signal into a set of time-domain basis functions with various frequency resolutions. Because of the simultaneous time–frequency decomposition of a signal, WT outperforms the traditional Fourier transform in effectively capturing the features of nonstationary signals. In conventional discrete wavelet transform and wavelet multiresolution analysis [51], however, only the scaling functions or approximations are decomposed into subspaces. The resulting time–frequency resolution has narrow bandwidths in the low frequencies and wide bandwidths in the high frequencies. It is not sufficient for discrimination between signals with close high-frequency components. Coifman and Wickerhauser [52] proposed the *discrete wavelet-packet transform* (DWPT) analysis to allow for a finer and adjustable resolution in the high frequencies (details). In wavelet-packet analysis, both scaling functions representing the approximations and wavelet functions representing the details are decomposed into subspaces. Therefore, WPT is a more effective approach than WT to extract features from either stationary or nonstationary signals [30,52].

On the other hand, directly using all wavelet transform coefficients for damage detection is tedious and may lead to inaccurate decisions. The wavelet-packet component energy (WPCE) measures the signal energy content contained in some specific frequency band. For given wavelet basis and decomposition level, the wavelet transform of a signal has been demonstrated to be unique and invariant [53,54]. Because the WPCE values extracted from the decomposed signals are also unique, they can be used as signal features to represent the system characteristic. The WPCE-based method has been demonstrated to be an effective feature representation of a signal in the context of condition monitoring of dynamic systems [55],

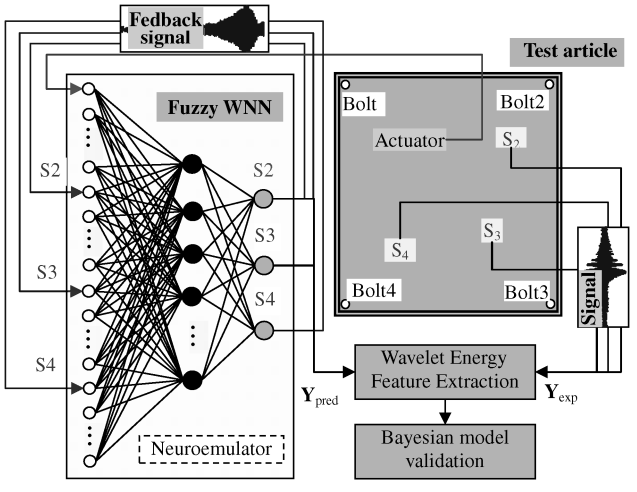

Fig. 4 Dynamic fuzzy wavelet neuroemulator for a TPS.

structural damage assessment [56], and incident detection in traffic patterns [57]. In this paper, the wavelet-packet component energy is used as the signal feature for model assessment and loosening detection.

In practical applications of the DWPT decomposition, a given time series with N data points $f(t)$ ($f(t) = y_i$ and $t = t_i$, where $i = 1, 2, \ldots, N$), is simultaneously decomposed into a series of scaling coefficients $s_j(k)$ and wavelet coefficients $w_j(k)$. The time series can then be represented by the inverse wavelet transform and the DWPT coefficients as follows:

$$\bar{f}(t) = \sum_{k\in Z}\sum_{j\in Z}[s_j(k)\psi_{j,k}(t) + w_j(k)\varphi_{j,k}(t)] \tag{2}$$

where the double summation indicates that the scaling and wavelet subspaces are simultaneously split into second-level subspaces to provide the frequency and time breakdown of the signal; $\varphi_{j,k}(t)$ is the wavelet function; $\psi_{j,k}(t)$ is the scaling function; k and j denote the time and the frequency indices, respectively; and Z is the set of all integers. The j-level scaling coefficients $s_j(k)$ and wavelet coefficients $w_j(k)$ are obtained by a recursive way for a given time series. Refer to Burrus et al. [58] for details of the DWPT decomposition.

The energy contribution from each DWPT component is mathematically expressed as a function of the wavelet and scaling coefficients as follows [58]:

$$E^f = \int_{-\infty}^{\infty} f^2(t)\mathrm{d}t = \sum_{m=1}^{2^j}\sum_{n=1}^{2^j}\int_{-\infty}^{\infty}|a_j^m(t)||a_j^n(t)|\mathrm{d}t \tag{3}$$

Using the orthogonal condition of wavelet functions, Eq. (3) becomes

$$E^f = \sum_{i=1}^{2^j} E_i^f = \sum_{i=1}^{2^j}\int_{-\infty}^{\infty}[a_j^i(t)]^2\mathrm{d}t \tag{4}$$

where $a_j^i(t)$ is the DWPT coefficient or component signal [$s_j(k)\psi_{j,k}(t)$ or $w_j(k)\varphi_{j,k}(t)$ in Eq. (2)], and E_i^f is the ith component energy stored in the corresponding component signal, which will be used for model validation and loosening detection in this paper.

B. Feature Assessment

We usually select the main energy components as features for model-validation and damage-detection purposes. Now we need to evaluate whether the selected components can be used to effectively represent the original signal. In this paper, the effectiveness of the selected feature packets is evaluated based on the reconstructed signal using two criteria: cross correlation and cross coherence.

The cross correlation between the reconstructed signal $\bar{f}(t)$ [i.e., Eq. (2)] and the original signal $f(t)$ is used to measure the similarity of the two signals in the time domain. Refer to [33] for the definition of the cross correlation between two signals. If there is no cross correlation between the two signals, then their cross correlation is constantly equal to zero, which is obviously not desirable. On the other hand, if $\bar{f}(t)$ is equal to $f(t)$, then their cross correlation is constantly equal to one. This case is also not desirable because it implies that the reconstructed signal completely represents the original one, including both the useful information and the noise. The desirable result is that the cross correlation approaches unity in the first few k, which implies that the constructed signal $\bar{f}(t)$ contains the useful information in $f(t)$ but not the noise.

The cross coherence between $\bar{f}(t)$ and $f(t)$ is used to measure the similarity of the two signals in the frequency domain. Again, refer to [33] for the definition of the cross coherence between two signals. The well-known Welch method [59] is used to estimate the power spectra density because it provides a smoothed spectral density estimate. Again, the cross coherence being close to 1 implies that the best selected features contain the useful information on the signal but not the noise.

V. Bayesian Evaluation Method

The developed fuzzy WNN model needs to be validated using the extracted features. Within the context of model validation, model outputs are compared with experimental observations to quantitatively assess the validity or predictive capabilities of computational models. Developing quantitative methods for model validation under uncertainty has become a problem of considerable research interest in recent years [33,42,44,45,60,61]. Statistical hypothesis testing is one approach to quantitative model validation under uncertainty, and both classic and Bayesian statistics have been explored. Refer to Babuska and Oden [60] and Oberkampf and Barone [61] for a comprehensive state-of-the-art review of various model-validation approaches.

On the other hand, the loose-bolt detection also involves comparing the model prediction (based on the original healthy condition of the test article) with the experimental result (representing the current condition of the test article). When the outputs predicted from the model are compared with the measured results (under the same input excitation), the difference between them will be used to detect the bolt-loosening (structural damage). Clearly, both model validation and damage detection involve comparing the model prediction with experimental observations. This paper implements a quantitative Bayesian approach for multivariate model assessment and loosening detection under uncertainty using the wavelet component-energy feature extracted from the time-series data.

Recently, an interval-based Bayesian hypothesis-testing method has been demonstrated to provide an effective tool for model validation [43]. Explicit expressions have been derived for calculating the validation metric based on the interval hypothesis testing in both univariate [45] and multivariate [33] cases. The method is employed in this research for multivariate model assessment and bolt-loosening detection of the test article.

Let $\mathbf{Y}_{\text{true}}$ be the feature for the (usually unknown) true response of the healthy test article (all bolts tightened fully) under the input excitation being considered at present; let $\mathbf{Y}_{\text{exp}}$ be the feature for the sensed response under the current (unknown) condition; and let $\mathbf{Y}_{\text{pred}}$ be the feature for the prediction output of the fuzzy WNN model representing structural responses under a healthy condition. [All three quantities ($\mathbf{Y}_{\text{true}}$, $\mathbf{Y}_{\text{exp}}$, and $\mathbf{Y}_{\text{pred}}$) are under the same input excitation.] Within the context of binary hypothesis testing, consider two hypotheses H_0 and H_1. Let $\mathbf{D} = \mathbf{Y}_{\text{exp}} - \mathbf{Y}_{\text{pred}}$ represent the difference between the measured data and the model prediction. Thus, model validation or loose-bolt detection becomes an interval-based hypothesis-testing problem, by defining the null hypothesis $H_0 : |\mathbf{D}| \le \boldsymbol{\varepsilon}$ (i.e., model is valid or structure is healthy) versus alternative hypothesis $H_1 : |\mathbf{D}| > \boldsymbol{\varepsilon}$ (i.e., model is inaccurate or structure is damaged), where $\boldsymbol{\varepsilon}$ is a predefined threshold vector and $|.|$ denotes the absolute value. Here, we are testing whether the difference $\mathbf{D}$ is within an allowable limit.

Assume that the difference $\mathbf{D}$ has a probability density function under each hypothesis: that is, $\mathbf{D}|H_0 \sim f(\mathbf{D}|H_0)$ and $\mathbf{D}|H_1 \sim f(\mathbf{D}|H_1)$. We do not know the distribution of the difference a priori, and so we assume Gaussian as an initial guess and then do a Bayesian update. We assume the following:

1) The difference $\mathbf{D}$ follows a multivariate normal distribution $N(\boldsymbol{\mu}, \boldsymbol{\Sigma})$ with the covariance matrix $\boldsymbol{\Sigma}$ obtained from the statistical analysis of the feature data available.

2) A prior density function of $\boldsymbol{\mu}$ under both null and alternative hypotheses, denoted by $f(\boldsymbol{\mu})$, is taken to be $N(\boldsymbol{\rho}, \boldsymbol{\Lambda}_0)$.

Using Bayes's theorem, $f(\boldsymbol{\mu}|\mathbf{D}) \propto f(\mathbf{D}|\boldsymbol{\mu})f(\boldsymbol{\mu})$, the Bayes factor for the multivariate case is equivalent to the volume ratio of the posterior density of $\boldsymbol{\mu}$ under two hypotheses, expressed as follows (Jiang and Mahadevan [33]):

$$B_M = \int_{-\boldsymbol{\varepsilon}}^{\boldsymbol{\varepsilon}} f(\boldsymbol{\mu}|\mathbf{D})\mathrm{d}\boldsymbol{\mu} \Big/ \left[\int_{-\infty}^{-\boldsymbol{\varepsilon}} f(\boldsymbol{\mu}|\mathbf{D})\mathrm{d}\boldsymbol{\mu} + \int_{\boldsymbol{\varepsilon}}^{\infty} f(\boldsymbol{\mu}|\mathbf{D})\mathrm{d}\boldsymbol{\mu}\right] = \frac{K}{1-K} \tag{5}$$

where the multivariate integral of

$$K = \int_{-\varepsilon}^{\varepsilon} f(\boldsymbol{\mu}|\mathbf{D})\mathrm{d}\boldsymbol{\mu}$$

is calculated by

$$\begin{aligned} K &= \int_{-\varepsilon\sqrt{n|\boldsymbol{\Lambda}|+|\boldsymbol{\Sigma}|}}^{\varepsilon\sqrt{n|\boldsymbol{\Lambda}|+|\boldsymbol{\Sigma}|}} (1/\sqrt{2\pi|\boldsymbol{\Pi}|}) \\ &\quad \times \exp\left[-\frac{1}{2}(\mathbf{Z}-\boldsymbol{\mu}_0)^T(\boldsymbol{\Pi})^{-1}(\mathbf{Z}-\boldsymbol{\mu}_0)\right]\mathrm{d}\mathbf{Z} \\ &\quad = \Phi(\boldsymbol{\varepsilon}_2, \boldsymbol{\mu}_0, \boldsymbol{\Pi}) - \Phi(\boldsymbol{\varepsilon}_1, \boldsymbol{\mu}_0, \boldsymbol{\Pi}) \end{aligned} \tag{6}$$

where $\Phi(.)$ presents a multivariate normal cumulative distribution function, which is computed in this paper using the numerical algorithm proposed by Genz [62], and

$$\boldsymbol{\varepsilon}_1 = -\boldsymbol{\varepsilon}\sqrt{n|\boldsymbol{\Lambda}_0| + |\boldsymbol{\Sigma}|} \tag{7}$$

$$\boldsymbol{\varepsilon}_2 = \boldsymbol{\varepsilon}\sqrt{n|\boldsymbol{\Lambda}_0| + |\boldsymbol{\Sigma}|} \tag{8}$$

$$\boldsymbol{\mu}_0 = (n\bar{\mathbf{D}}|\boldsymbol{\Lambda}_0| + \boldsymbol{\rho}|\boldsymbol{\Sigma}|)/\sqrt{n|\boldsymbol{\Lambda}_0| + |\boldsymbol{\Sigma}|} \tag{9}$$

$$\boldsymbol{\Pi} = \boldsymbol{\Sigma}|\boldsymbol{\Lambda}_0| \tag{10}$$

where $|.|$ denotes the determinant of a matrix, and the value of $\bar{\mathbf{D}}$ is calculated from the difference of the feature data between $\mathbf{Y}_{\text{exp}}$ and $\mathbf{Y}_{\text{pred}}$; that is,

$$\bar{\mathbf{D}} = \frac{1}{n}\sum_{i=1}^{n}\mathbf{D}_i$$

Refer to Jiang and Mahadevan [33] for details of the derivation of the preceding formulas.

Five issues need to be pointed out regarding the Bayesian method. First, if no information on $f(\boldsymbol{\mu}|H_1)$ is available, the parameters $\boldsymbol{\rho} = \mathbf{0}$ and $\boldsymbol{\Lambda}_0 = \boldsymbol{\Sigma}$ are suggested by Migon and Gamerman [63]. This selection assumes that the amount of information in the prior $\boldsymbol{\mu}$ is equal to that in the observation, which is consistent with the Fisher information-based method [64]. Thus, the parameters in Eqs. (7–10) can be simplified as

$$\boldsymbol{\varepsilon}_1 = -\boldsymbol{\varepsilon}\sqrt{(n+1)|\boldsymbol{\Sigma}|}, \qquad \boldsymbol{\varepsilon}_2 = \boldsymbol{\varepsilon}\sqrt{(n+1)|\boldsymbol{\Sigma}|}$$
$$\boldsymbol{\mu}_0 = n\bar{\mathbf{D}}\sqrt{|\boldsymbol{\Sigma}|}/\sqrt{n+1}, \qquad \boldsymbol{\Pi} = \boldsymbol{\Sigma}|\boldsymbol{\Sigma}|$$

Second, the quantity K in Eq. (6) is dependent on the value of ε. The decision maker or model user has to decide what value of ε is acceptable. For the sake of illustration, the value of ε is always taken to be 0.5 times the standard deviation of each variable in the numerical example presented in Sec. VI.

Third, because B_M is nonnegative, the value of B_M can be converted to the logarithmic scale for convenience of comparison among a larger range of values [i.e., $b_M = \ell_n(B_M)$]. Kass and Raftery [64] suggested interpreting b_M between 0 and 1 as weak evidence in favor of H_0, between 3 and 5 as strong evidence, and $b_M > 5$ as very strong evidence. Negative b_M of the same magnitude is said to favor H_1 by the same amount.

Fourth, the current work is based on the Gaussian error assumption. In the case of nonnormality, various transformation methods [65] are available to achieve normality of error data. The transformed data can then be used in the Bayesian methodology for model validation and bolt-loosening detection. Refer to Rebba and Mahadevan [43] for details of the transformation of nonnormality to normality.

Fifth, and finally, assume the prior probabilities of two hypotheses to be $Pr(H_0) = 0.5$ and $Pr(H_1) = 0.5$ in the absence of prior knowledge of each hypothesis before testing. Then the confidence in the model based on the validation data or the confidence in the healthy status of the test article based on the detection data can be quantified as [42]

$$\kappa = Pr(H_0|\text{data}) = B_M/(B_M + 1) \tag{11}$$

where κ is a measure of confidence in the range of 0–100%. Obviously, from Eq. (11), $B_M \to 0$ indicates 0% confidence in accepting the model, and $B_M \to \infty$ indicates 100% confidence.

Furthermore, to consider the uncertainties in both measured data and model prediction, we treat the Bayes factor B_M as a random variable. Given the probability density function of ε_{obs}, M sets of mean $\bar{\varepsilon}$ and sum of squared errors s values are created by sampling m error data using Monte Carlo simulation ($m = 5000$ and $M = 5000$ are taken in this paper). The resulting B_M values by Eq. (5) are used to construct its probability density function. Then the probability of the event that either the model is acceptable or the structure is healthy (i.e., accepting the null hypothesis) can be estimated by finding the proportion of $b_{01} > 0$: that is, $\gamma = Pr(b_{01} > 0)$. Thus, the stochastic approach directly provides a quantitative probability of accepting the model in terms of model validation or a loose bolt in terms of damage detection.

VI. Numerical Implementation

The dynamic fuzzy WNN model is constructed using the measured input–output data collected from the healthy test article with all four bolts fully tightened and then trained using the adaptive LM-LS algorithm, as described by Jiang and Adeli [27] and Adeli and Jiang [32]. In training the model, the excitation signal at S_1 and the response signals collected by sensors S_2, S_3, and S_4 during the previous three time intervals {$D = 4 \times 3$ in Eq. (1), as explained in Adeli and Jiang [26,32]} are used as multiple inputs, and the current response signals at S_2, S_3, and S_4 are used as multiple outputs of the model. The trained model is then used to represent the structural system and to predict the responses at the three sensed locations of the test article under the seven sensor configurations shown in Table 1.

Note that in practical implementation, we usually need only one set of experimental data to train the model to capture the dynamic characteristics of the underlying system. In this study, we make full use of the existing data sets. In each sensor configuration, the first 20 sets of sensor data collected from the test article under the healthy condition is selected and used to train the model. Each trained model is tested using the remaining 30 sets of sensed data under the healthy condition. Thus, seven different sets of system-identification results are produced to represent the seven sensor configurations. As an example, Fig. 5 shows the time-series plots and absolute error of system-identification results for the 25th data set in configuration 1 from 1.5 to 2.0 s. An enlarged graph is embedded in this figure for comparison purposes. Clearly, it is difficult to graphically distinguish the difference between two data sets, implying that the trained model may be acceptable to represent the structural system.

In the following subsections, both predicted and measured time histories are decomposed using the four-level discrete wavelet-packet transform method. Then wavelet-packet component energy is computed as the signal feature at every decomposition node at the fourth level. The principal energy contents that dominate the signal energy are used to construct multivariate data sets for both model validation and loose-bolt detection. The effectiveness of the selected feature is assessed using both cross-correlation and cross-coherence metrics. The multivariate problems are handled by interval-based Bayesian hypothesis testing, followed by a probabilistic assessment for model validation and damage detection.

A. Wavelet-Packet Component Energy

Using a Daubechies wavelet of order 5, the four-level DWPT decompositions [$j = 4$ in Eq. (2)] are performed on all response

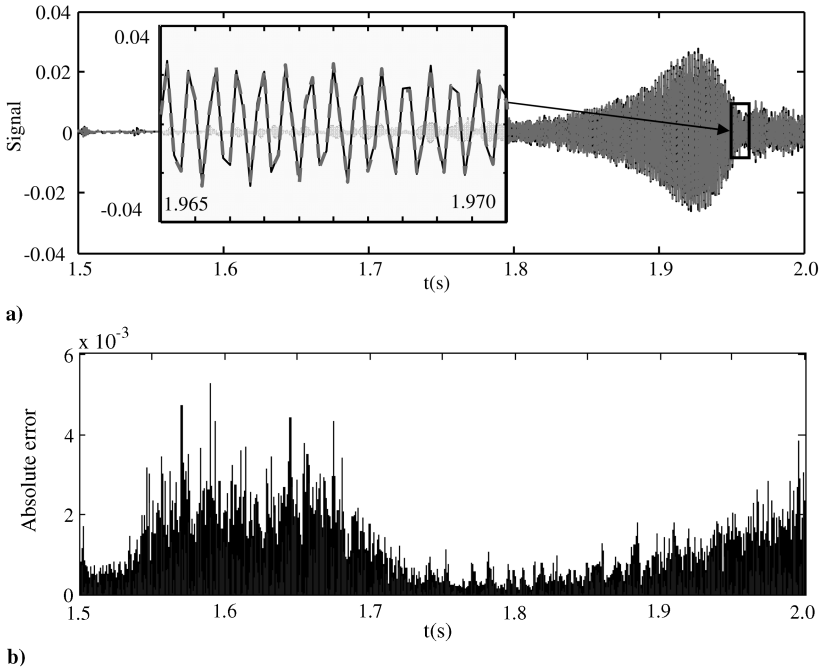

Fig. 5 System-identification results of 25th data set for sensor 2 in configuration 1 from 1.5 to 2.0 s: a) time-series plot, and b) absolute error.

time–history data, in the context of both model validation and loosening detection. Every set of data is resolved into 16 (2^j) series corresponding to the 16 decomposition subspaces at the fourth level. Next, using Eq. (3), the component energy E_i^f is calculated for every set of decomposed coefficient at the fourth level, resulting in 16 energy values from every set of response data. We sort the energy values in descending order and find that more than 98% signal energy is stored in the first 7 sorted wavelet-packet component-energy values. As an example, Fig. 6 shows the wavelet energy percentage of four-level DWPT decomposition coefficients for both measured and predicted response series for the 25th data set of sensor 2 in configuration 1 under a 1) healthy condition (i.e., all four bolts fully tightened) and 2) damaged condition (i.e., 25% nominal torque of bolt 1).

The cross correlation and cross coherence between the original signal and the reconstructed signal using the first seven wavelet packets are computed for both measured data and model prediction of each test. It is observed that both cross-correlation and cross-coherence values approach unity for the first few time delays, implying that the first seven feature values (i.e., wavelet-packet component energy) are enough to represent the original signal. As an example, Fig. 7 shows the assessment results of both measured data

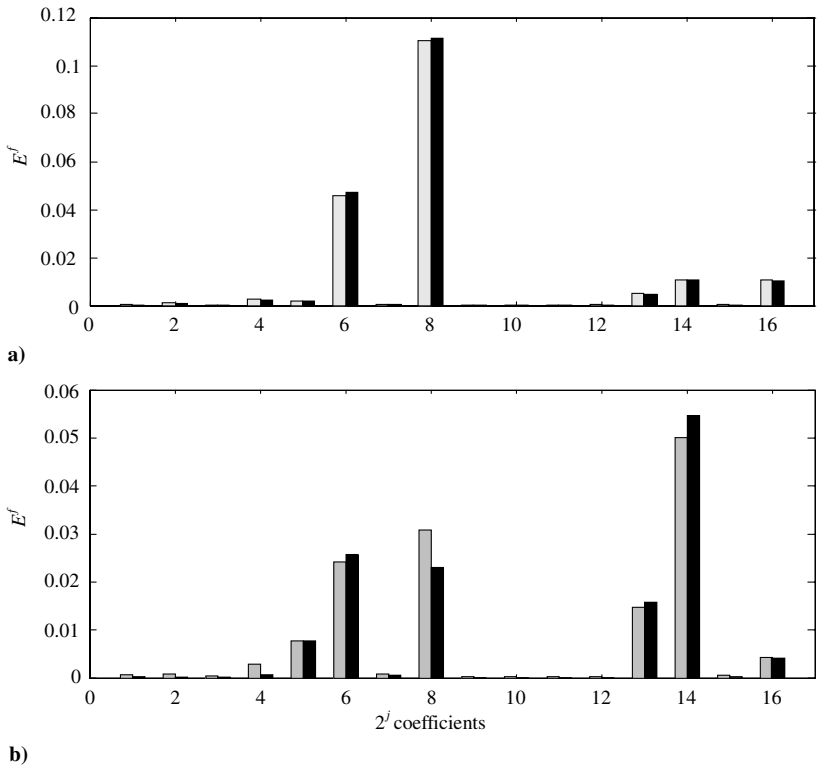

Fig. 6 Wavelet energy percentage of four-level DWPT decomposition coefficients ($j = 4$) for the 25th data set of sensor 2 (model validation): a) healthy condition ($E_7 = 98.7\%$) and b) damaged condition ($E_7 = 99.1\%$); E_7 is the summation of the first seven maximum wavelet energy values of the predicted signal; □ denotes experimental data and ■ denotes model prediction

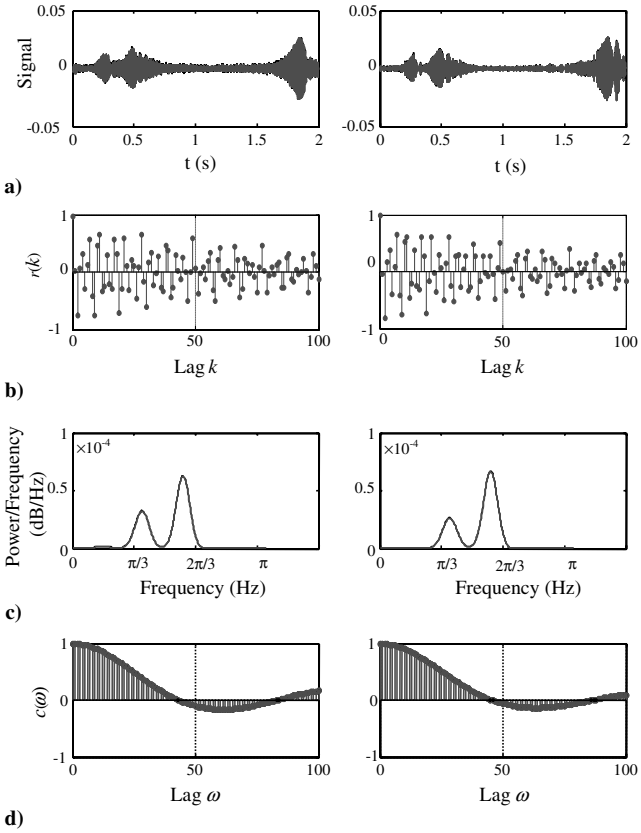

Fig. 7 Assessment of response signals reconstructed using seven wavelet packets with maximum wavelet energy values shown in Fig. 6 (left column: experimental data; right column: model prediction): a) time-series plots, b) cross-correlation of signals, c) power spectra density using Welch's method, and d) cross coherence of signals.

and model prediction reconstructed using the first seven wavelet packets for the 25th test of sensor 2 at configuration 1 under a healthy condition. Thus, only the first seven feature values are used as the measure of a signal to compare the predicted and measured time series, resulting in a 7-variable model validation and loosening detection problem for the test article.

B. Model Validation

Note that one set of data has been arbitrarily selected from the 50 sets of sensor data collected from the test article under the healthy condition and used to construct and train the fuzzy WNN model, as described previously. Therefore, in the context of model validation, we can construct a $3 \times 7 \times 30$ matrix $\mathbf{D}$ for each configuration using the remaining 30 sets of validation data, which represents 3 sensor locations, each having 7 variables and each variable having 30 values of the difference of wavelet-packet component energy between the measured and predicted response acceleration data. For each sensor, the 7-variable model-validation problem becomes the testing of whether the set of means $\bar{\mathbf{D}}$ are within an allowable limit.

To apply the Bayesian methods described in Sec. V, a multivariate normal distribution is used to model these data. For each sensor, using the statistics of the seven component-energy variables obtained from the 30 sets of data (i.e., the number of experiments $n = 30$), the Bayes factor values are calculated by the Bayesian interval hypothesis-testing method [Eq. (5)] for each configuration shown in Table 1. The acceptance confidence $k = B_M/(B_M + 1)$ is also obtained using Eq. (11) for all cases. The computed results are summarized in Table 2. Note that the value in Table 2 is the Bayes factor in the logarithmic scale [i.e., $b_M = \ell_n(B_M)$] for the convenience of comparison. It is indicated that all b_M have a quite large value (greater than 3) with a relatively high probability of accepting the model (i.e., $\kappa > 96\%$). The results demonstrate that the models in all seven configurations have been well trained and are acceptable for bolt-loosening detection based on the Bayesian assessment results.

Furthermore, the statistics of errors of the seven energy variables for each sensor and each configuration are used to perform the probabilistic assessment of model validity. The 5000 simulations are run for each case using Monte Carlo technique. The densities of $b_M = \ell_n(B_M)$ are then estimated using the smoothing method based on a kernel normal function [66]. For each case, the probability of accepting the model [i.e., $\gamma = \text{prob}(b_M > 0)$] is also obtained by finding the proportion of $b_M > 0$. All of the results are also summarized in Table 2. As an example, Fig. 8 shows the simulated results of b_M for sensor 2 at various configurations under healthy condition. Two observations are obtained from the probabilistic assessment results. First, the probability of accepting the model is larger than 96% for all cases, implying that all models are accepted based on the probabilistic assessment results as well. Second, the probability of accepting the model (γ) is close to that (κ) obtained using the experimental data for each case. This is expected, because each κ value in the Bayesian assessment is obtained from 30 experimental data individually. The numerical results indicate that the sample size of $n = 30$ is enough to quantify the uncertainty in the experimental data.

C. Loose-Bolt Detection

In the context of bolt-loosening detection, each validated model is used to predict the responses of the test article under the damage condition (bolt 1 with only 25% nominal torque). We can construct a $3 \times 7 \times 50$ matrix $\mathbf{D}$, in which all 50 sets of sensed data are used in the detection.

Again, a multivariate normal distribution is used to model these data. Similar to model validation, using the statistics of seven component-energy variables obtained from the 50 sets of energy difference data (i.e., the number of experiments $n = 50$ in this case) for each sensor, the Bayes factor values are calculated by the Bayesian interval-based method [Eq. (5)] for each configuration shown in Table 1. The acceptance confidence κ is also obtained using Eq. (11) for all cases. All results are summarized in Table 3. As before, the b_M value in Table 3 is the Bayes factor in the logarithmic scale.

In Table 3, the negative Bayes factor value b_M indicates that there exists at least one loose bolt in the test article, with the probability of detection of $1 - \kappa$. The location of the loose bolt may be identified based on the magnitude of b_M or $1 - \kappa$ of the three sensors for each configuration. For example, in addition to the sixth configuration with $b_M = 2.394$ for S_3, all b_M values of sensor 3 for the other six configurations are larger than 3, which strongly supports ($\kappa > 97\%$)

Table 2 Model-validation results

	S_2			S_3			S_4		
Configuration	b_{M2}	κ_2, %	γ_2, %	b_{M3}	κ_3, %	γ_3, %	b_{M4}	κ_4, %	γ_4, %
1	15.11	100.0	97.5	7.954	100.0	99.9	6.311	99.8	98.0
2	4.191	98.5	98.2	4.108	98.4	97.5	6.161	99.8	97.3
3	3.265	96.3	97.7	3.754	97.7	99.2	4.421	98.8	98.1
4	5.178	99.4	99.2	5.954	99.7	99.0	12.58	100.0	99.0
5	7.321	99.9	98.1	17.99	100.0	100.0	8.673	100.0	100.0
6	18.31	100.0	96.5	3.381	96.7	98.8	5.813	99.7	97.8
7	11.38	100.0	97.4	6.686	99.9	98.6	7.725	100.0	100.0

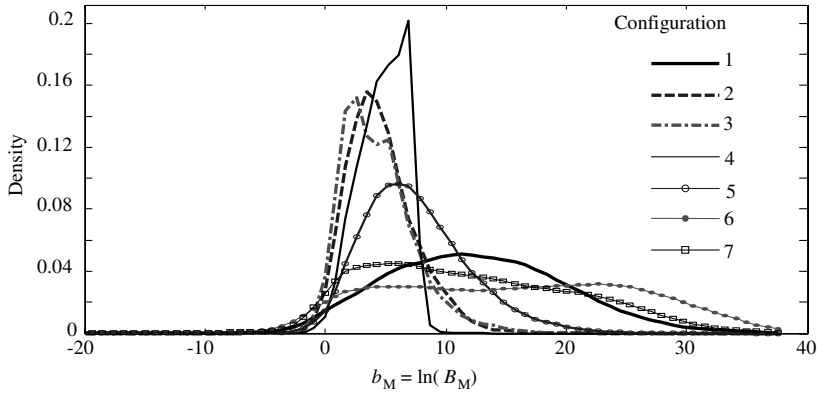

Fig. 8 Simulated results of $b_M = \ell_n(B_M)$ for sensor 2 at various configurations under a healthy condition: the densities are kernel density estimates based on samples of size 5000 from the respective densities; at all seven configurations, the probability of accepting the model is $\gamma = \text{prob}(b_M > 0) > 96\%$.

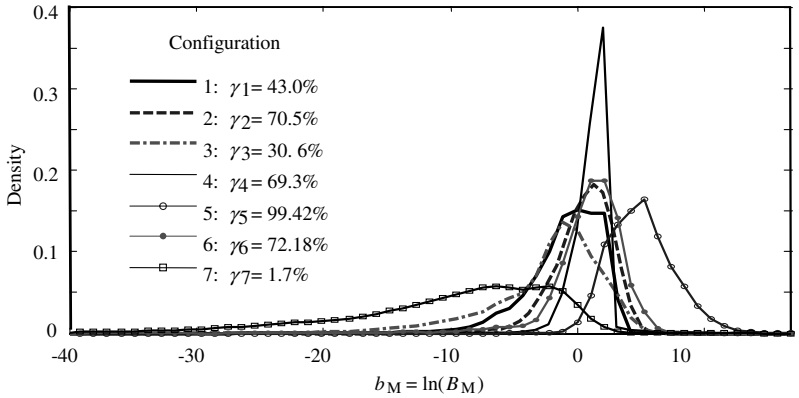

Fig. 9 Simulated results of $b_M = \ell_n(B_M)$ for sensor 2 in various configurations under a damaged condition: the densities are kernel density estimates based on samples of size 5000 from the respective densities; the probabilities of no loose-bolt $\gamma = \text{prob}(b_M > 0)$ are shown.

the conclusion that the bolt near sensor 3 (i.e., bolt 3) is tightened. In addition, the b_M values of all three sensors for configuration 5 are larger than 3, which strongly supports the conclusion that only bolt 1 is possibly loosened in this configuration, if any.

Again, the statistics of errors of the seven energy variables for each sensor and each configuration are used to perform the probabilistic assessment of bolt 1 loosening. The 5000 simulations are run for each case using Monte Carlo technique. The densities of b_M are then estimated using the smoothing method based on a kernel normal function. For each case, the probability of $b_M > 0$ is obtained by finding its proportion. All of the results are also summarized in Table 3. As an example, Fig. 9 shows the simulated results of b_M for sensor 2 at various configurations under damaged condition.

VII. Conclusions

This paper presents a wavelet energy-based Bayesian methodology to detect loose bolts in thermal protection system panels of space vehicles. A dynamic fuzzy wavelet neural-network model is employed to perform the multiple-input/multiple-output nonparametric system identification. The nonparametric model is trained using the data collected from a test article under a healthy condition, and the trained model is then used to predict dynamic responses of the healthy test article under an unknown condition, thus reducing experimental expense by avoiding tests of the healthy article under various excitations. Both predicted and observed time histories are decomposed using the discrete wavelet-packet transform method, and the computed wavelet-packet component energy is used as the signal feature to construct a multivariate problem for model validation and bolt-loosening detection. The effectiveness of the selected feature is assessed using both cross-correlation and cross-coherence metrics. The multivariate problems are handled by the interval-based Bayesian hypothesis-testing method, followed by a probabilistic assessment for model validation and loose-bolt detection. This study is targeted toward an active online health-monitoring system for loose-bolt detection in a TPS panel.

The Bayesian wavelet methodology is investigated with a simplified TPS component with experimental structural response data collected from both healthy and damaged (one bolt loose) states using an active sensing system. Several conclusions are obtained from the numerical results. First, the detectability of a loose bolt largely depends on the location of sensors. As shown in Table 3, the

Table 3 Damage-detection results

	S_2			S_3			S_4		
Configuration	b_{M2}	κ_2, %	γ_2, %	b_{M3}	κ_3, %	γ_3, %	b_{M4}	κ_4, %	γ_4, %
1	−0.271	43.3	43.0	4.926	99.3	97.7	−1.811	14.1	28.3
2	0.904	71.2	70.5	5.130	99.4	96.7	4.724	99.1	97.5
3	−1.502	18.2	30.6	8.327	100	93.9	5.732	99.7	99.5
4	0.245	56.1	69.3	6.772	99.9	99.5	−0.748	32.1	30.6
5	4.647	99.1	99.4	5.587	99.6	99.9	3.503	97.1	95.9
6	1.878	86.7	72.2	2.394	91.6	87.7	−1.886	13.2	11.2
7	−8.532	0.02	1.7	3.821	97.9	93.4	2.455	92.1	92.1

probability of successfully detecting a loose bolt varies with the sensor configuration. Second, the uncertainties in both sensed data and model prediction are incorporated in the Bayesian hypothesis testing. Third, and finally, the probabilistic methodology provides an efficient measure to quantify the confidence in the damage detection.

Note that the present methodology makes use of the known excitation signal in the numerical example. The methodology may be slightly modified for the scenarios with unknown excitations. Please refer to Jiang and Adeli [28,29] and Adeli and Jiang [32] for details about the formulation and validation without input excitations. The current implementation of the proposed methodology is based on the assumption that only one bolt is loose in the thermal protection system panel. Future study needs to investigate the more complicated case of simultaneous damage in multiple bolts. In addition, this methodology will be extended to isolate the location of the loose bolt and to identify the loosening extent, by combining with statistical feature selection and classification.

Acknowledgments

The study reported in this paper was supported by funds from Sandia National Laboratories, Albuquerque, New Mexico (contract no. BG-7732, project monitors Thomas L. Paez, Laura P. Swiler, and Martin Pilch). The support is gratefully acknowledged. In addition, the experiments on the prototype test article were sponsored by the U.S. Air Force Research Laboratory (project monitor Mark Derriso) through subcontract to Anteon Corporation. The authors gratefully appreciate this support.

References

[1] Lovell, P. A., and Pines, D. J., "Damage Assessment in a Bolted Lap Joint," *Smart Structures and Materials 1998: Smart Systems for Bridges, Structures, and Highways*, Proceedings of SPIE, Vol. 3325, Society of Photo-Optical Instrumentation Engineers, Bellingham, WA, 1998, pp. 112–126.doi:10.1117/12.310600

[2] Housner, G. W., Bergman, L. A., Caughey, T. K., Chassiakos, A. G., Claus, R. O., Masri, S. F., Skelton, R. E., Soong, T. T., Spencer, B. F., and Yao, J. T. P., "Structural Control: Past, Present, and Future," *Journal of Engineering Mechanics*, Vol. 123, No. 9, 1997, pp. 897–971.
doi:10.1061/(ASCE)0733-9399(1997)123:9(897)

[3] Aktan, A. E., Farhey, D. N., Helmicki, A. J., Brown, D. L., Hunt, V. J., Lee, K. L., and Levi, A., "Structural Identification for Condition Assessment: Experimental Arts," *Journal of Structural Engineering*, Vol. 123, No. 12, 1997, pp. 1674–1684.
doi:10.1061/(ASCE)0733-9445(1997)123:12(1674)

[4] Catbas, F. N., and Aktan, A. E., "Condition and Damage Assessment: Issues and Some Promising Indices," *Journal of Structural Engineering*, Vol. 128, No. 8, 2002, pp. 1026–1038.
doi:10.1061/(ASCE)0733-9445(2002)128:8(1026)

[5] Chong, K. P., Carino, N. J., and Washer, G., "Health Monitoring of Civil Infrastructures," *Smart Materials and Structures*, Vol. 12, No. 3, 2003, pp. 483–493.
doi:10.1088/0964-1726/12/3/320

[6] Wood, K. H., Brown, T. L., Wu, M. C., and Gause, C. B., "Fiber Optic Sensors for Cure/Health Monitoring of Composite Materials," *Proceeding of the 3rd International Workshop on Structural Health Monitoring*, CRC Press, Boca Raton, FL, 2001.

[7] Prosser, W. H., Brown, T. L., Woodard, S. E., Fleming, G. A., and Cooper, E. G., "Sensor Technology for Integrated Vehicle Health Management of Aerospace Vehicles," *AIP Conference Proceedings*, Vol. 657, No. 1, Mar. 2003, pp. 1582–1589.
doi:10.1063/1.1570319

[8] Staszewski, W. J., Boller, C., Grondel, S., Biemans, C., O'Brien, E., Delebarre, C., and Tomlinson, G. R., "Damage Detection Using Stress and Ultrasonic Waves," *Health Monitoring of Aerospace Structures*, edited by W. J. Staszewski, C. Boller, and G. R. Tomlinson, Wiley, Hoboken, NJ, 2004.

[9] Forth, S. C., and Staroselsky, A., "Fracture Evaluation of In-Situ Sensors for High Temperature Applications," *Proceedings of the 10th International Congress of Fracture* [CD-ROM], NASA Center for AeroSpace Information, Hanover, MD, 2001.

[10] Blackshire, J. L., Giurgiutiu, V., Cooney, A., and Doane, J., "Characterization of Sensor Performance and Durability for Structural Health Monitoring Systems," *Advanced Sensor Technologies for Nondestructive Evaluation and Structural Health Monitoring*, Proceedings of SPIE, Vol. 5770, Society of Photo-Optical Instrumentation Engineers, Bellingham, WA, 2005, pp. 66–75.
doi:10.1117/12.599888

[11] Blackshire, J. L., and Cooney, A., "Characterization of Bonded Piezoelectric Sensor Performance and Durability in Simulated Aircraft Environments," *AIP Conference Proceedings*, Vol. 820, 2006, pp. 1694–1701.
doi:10.1063/1.2184725.

[12] Blackshire, J. L., and Cooney, A., "Evaluation and Improvement in Sensor Performance and Durability for Structural Health Monitoring Systems," *Advanced Sensor Technologies for Nondestructive Evaluation and Structural Health Monitoring II*, Proceedings of SPIE, Vol. 6179, Society of Photo-Optical Instrumentation Engineers, Bellingham, WA, 2006, Paper 61790K.
doi:10.1117/12.659024

[13] Paté-Cornell, E., and Fischbeck, P. S., "Probabilistic Risk Analysis and Risk-Based Priority Scale for Tiles of the Space Shuttle," *Reliability Engineering and System Safety*, Vol. 40, No. 3, 1993, pp. 221–238.
doi:10.1016/0951-8320(93)90062-4

[14] Park, G., Cudney, H. H., and Inman, D. J., "An Integrated Health Monitoring Technique Using Structural Impedance Sensors," *Journal of Intelligent Material Systems and Structures*, Vol. 11, No. 6, 2000, pp. 448–455.
doi:10.1106/QXMV-R3GC-VXXG-W3AQ

[15] DeSimio, M., Miller, I., Derriso, M., Brown, K., and M. Baker, "Structural Health Monitoring Experiments with a Canonical Element of an Aerospace Vehicle," *Proceedings of the 2003 IEEE Aerospace Conference*, Vol. 7, Inst. of Electrical and Electronics Engineers, Piscataway, NJ, Mar. 2003, pp. 3105–3111.

[16] Derriso, M. M., Braisted, W., Rosenstengel, J., and DeSimio, M., "The Structural Health Monitoring of a Mechanically Attached Thermal Protection System," *JOM*, Vol. 56, No. 3, 2004, pp. 36–39.
doi:10.1007/s11837-004-0030-9

[17] Peairs, D. M., Park, G., and Inman, D. I., "Improving Accessibility of the Impedance-Based Structural Health Monitoring Method," *Journal of Intelligent Material Systems and Structures*, Vol. 15, No. 2, 2004, pp. 129–139.
doi:10.1177/1045389X04039914

[18] Peairs, D. M., Park, G., and Inman, D. I., "Practical Issues of Activating Self-Repairing Bolted Joints," *Smart Materials and Structures*, Vol. 13, No. 6, 2004, pp. 1414–1423.
doi:10.1088/0964-1726/13/6/012

[19] Yang, J., and Chang, F.-K., "Verification of a Built-In Health Monitoring System for Bolted Thermal Protection Panels," *Smart Structures and Materials 2005*, Proceedings of SPIE, Vol. 5765, 2005, pp. 769–780.
doi:10.1117/12.600213

[20] Yang, J., and Chang, F.-K., "Detection of Bolt-Loosening in C-C Composite Thermal Protection Panels 1: Diagnostic Principle," *Smart Materials and Structures*, Vol. 15, No. 2, 2006, pp. 581–590.
doi:10.1088/0964-1726/15/2/041

[21] Yang, J., and Chang, F.-K., "Detection of Bolt-Loosening in C-C Composite Thermal Protection Panels 2: Experimental Verification," *Smart Materials and Structures*, Vol. 15, No. 2, 2006, pp. 591–599.
doi:10.1088/0964-1726/15/2/042

[22] Sohn, H., Farrar, C. R., Hunter, N. F., and Worden, K., "Structural Health Monitoring Using Statistical Pattern Recognition Techniques," *Journal of Dynamic Systems, Measurement, and Control*, Vol. 123, No. 4, 2001, pp. 706–711.
doi:10.1115/1.1410933

[23] Sohn, H., Farrar, C. R., Hemez, F. M., Shunk, D. D., Stinemates, D. W., and Nadler, B. R., "A Review of Structural Health Monitoring Literature: 1996–2001," TR LA-13976-MS, Los Alamos National Lab., Los Alamos, NM, 2003.

[24] Nichols, J. M., Nichols, C. J., Todd, M. D., Seaver, M., Trickey, S. T., and Virgin, L. N., "Use of Data-Driven Phase Space Models in Assessing the Strength of a Bolted Connection in a Composite Beam," *Smart Materials and Structures*, Vol. 13, No. 2, 2004, pp. 241–250.
doi:10.1088/0964-1726/13/2/001

[25] Hundhausen, R. J., Adams, D. E., Derriso, M., Kukuchek, P., and Alloway, R., "Loads, Damage Identification and NDE/SHM Data Fusion in Standoff Thermal Protection Systems Using Passive Vibration-Based Methods," *Second European Workshop on Structural Health Monitoring*, DEStech, Lancaster, PA, 2004, pp. 959–966.

[26] Adeli, H., and Jiang, X., "Dynamic Fuzzy Wavelet Neural Network Model for Structural System Identification," *Journal of Structural Engineering*, Vol. 132, No. 1, 2006, pp. 102–111.
doi:10.1061/(ASCE)0733-9445(2006)132:1(102)

[27] Jiang, X., and Adeli, H., "Dynamic Wavelet Neural Network for Nonlinear System Identification," *Computer-Aided Civil and Infrastructure Engineering*, Vol. 20, No. 5, 2005, pp. 316–330. doi:10.1111/j.1467-8667.2005.00399.x

[28] Jiang, X., and Adeli, H., "Psuedospectra, MUSIC, and Dynamic Wavelet Neural Network for Damage Detection of High-Rise Buildings," *International Journal for Numerical Methods in Engineering*, Vol. 71, No. 5, 2007, pp. 606–629. doi:10.1002/nme.1964

[29] Jiang, X., and Adeli, H., "Dynamic Fuzzy Wavelet Neuroemulator for Active Nonlinear Control of Structures," *International Journal for Numerical Methods in Engineering*, Vol. 74, No. 7, 2008, pp. 1045–1066. doi:10.1002/nme.2195

[30] Jiang, X., Mahadevan, S., and Adeli, H., "Bayesian Wavelet Packet Denoising for Structural System Identification," *Structural Control and Health Monitoring*, Vol. 14, No. 2, 2007, pp. 333–356. doi:10.1002/stc.161

[31] Jiang, X., and Mahadevan, S., "Bayesian Wavelet Methodology for Structural Damage Detection," *Structural Control and Health Monitoring*, Vol. 15, No. 7, 2008, pp. 974–991. doi:10.1002/stc.230

[32] Adeli, H., and Jiang, X., *Intelligent Infrastructure: Neural Networks, Wavelets, and Chaos Theory for Intelligent Transportation Systems and Smart Structures*, CRC Press, Boca Raton, FL, 2008.

[33] Jiang, X., and Mahadevan, S., "Bayesian Wavelet Method for Multivariate Model Assessment of Dynamical Systems," *Journal of Sound and Vibration*, Vol. 312, Nos. 4–5, 2008, pp. 694–712. doi:10.1016/j.jsv.2007.11.025

[34] Kittler, J., "Mathematics Methods of Feature Selection in Pattern Recognition," *International Journal of Man-Machine Studies*, Vol. 7, No. 5, 1975, pp. 609–637. doi:10.1016/S0020-7373(75)80023-X

[35] Chen, M. H., Lee, D., and Pavlidis, T., "Residual Analysis for Feature Detection," *IEEE Transactions on Pattern Analysis and Machine Intelligence*, Vol. 13, No. 1, 1991, pp. 30–40. doi:10.1109/34.67628

[36] Cho, Y. S., Kim, S. B., Hixson, E. L., and Powers, E. J., "A Digital Technique to Estimate Second-Order Distortion Using Higher Order Coherence Spectra," *IEEE Transactions on Signal Processing*, Vol. 40, No. 5, 1992, pp. 1029–1040. doi:10.1109/78.134466

[37] Rioul, O., and Flandrin, P., "Time-Scale Energy Distributions: A General Class Extending Wavelet Transforms," *IEEE Transactions on Signal Processing*, Vol. 40, No. 7, 1992, pp. 1746–1757. doi:10.1109/78.143446

[38] Ornstein, D. S., and Weiss, B., "Entropy and Data Compression Schemes," *IEEE Transactions on Information Theory*, Vol. 39, No. 1, 1993, pp. 78–83. doi:10.1109/18.179344

[39] Wu, Y., and Du, R., "Feature Extraction and Assessment Using Wavelet Packets for Monitoring of Machining Processes," *Mechanical Systems and Signal Processing*, Vol. 10, No. 1, 1996, pp. 29–53. doi:10.1006/mssp.1996.0003

[40] Yan, R., and Gao, R. X., "An Efficient Approach to Machine Health Diagnosis Based on Harmonic Wavelet Packet Transform," *Robotics and Computer-Integrated Manufacturing*, Vol. 21, Nos. 4–5, 2005, pp. 291–301. doi:10.1016/j.rcim.2004.10.005

[41] Zhang, R., and Mahadevan, S., "Bayesian Methodology for Reliability Model Acceptance," *Reliability Engineering and System Safety*, Vol. 80, No. 1, 2003, pp. 95–103. doi:10.1016/S0951-8320(02)00269-7

[42] Mahadevan, S., and Rebba, R., "Validation of Reliability Computational Models Using Bayes Networks," *Reliability Engineering and System Safety*, Vol. 87, No. 2, 2005, pp. 223–232. doi:10.1016/j.ress.2004.05.001

[43] Rebba, R., and Mahadevan, S., "Model Predictive Capability Assessment Under Uncertainty," *AIAA Journal*, Vol. 44, No. 10, 2006, pp. 2376–2384. doi:10.2514/1.19103

[44] Jiang, X., and Mahadevan, S., "Bayesian Risk-Based Decision Method for Model Validation Under Uncertainty," *Reliability Engineering and System Safety*, Vol. 92, No. 6, 2007, pp. 707–718. doi:10.1016/j.ress.2006.03.006

[45] Jiang, X., and Mahadevan, S., "Bayesian Validation Assessment of Multivariate Computational Models," *Journal of Applied Statistics*, Vol. 35, No. 1, 2008, pp. 49–65. doi:10.1080/02664760701683577

[46] Olson, S., DeSimio, M., and Derriso, M., "Fastener Damage Estimation in a Square Aluminum Plate," *Structural Health Monitoring*, Vol. 5, No. 2, 2006, pp. 173–183. doi:10.1177/1475921706058007

[47] Guratzsch, R. F., and Mahadevan, S., "Probabilistic Optimization of Sensor Placement," *Proceedings of the IMAC XXV Conference and Exposition on Structural Dynamics* [CD-ROM], Society for Experimental Mechanics, Bethel, CT, 2007.

[48] Guratzsch, R. F., and Mahadevan, S., "Health Monitoring Sensor Placement Optimization Under Uncertainty," 11th AIAA/ISSMO Multidisciplinary Analysis and Optimization Conference, Portsmouth, VA, AIAA Paper 2006-7034, Sept. 2006.

[49] Bezdek, J. C., *Pattern Recognition with Fuzzy Objective Function Algorithms*, Plenum, New York, 1981.

[50] Chatfield, C., *The Analysis of Time Series: an Introduction*, 6th ed., Chapman & Hall/CRC, Boca Raton, FL, 2004.

[51] Percival, D. B., and Walden, A. T., *Wavelet Methods for Time Series Analysis*, Cambridge Univ. Press, New York, 2000.

[52] Coifman, R. R., and Wickerhauser, M. V., "Entropy-Based Algorithms for Best Basis Selection," *IEEE Transactions on Information Theory*, Vol. 38, No. 2, 1992, pp. 713–718. doi:10.1109/18.119732

[53] Daubechies, I., "Orthonormal Bases of Compactly Supported Wavelets," *Communications on Pure and Applied Mathematics*, Vol. 41, No. 7, 1988, pp. 909–996. doi:10.1002/cpa.3160410705

[54] Mallat, S., "A Theory for Multiresolution Signal Decomposition: The Wavelet Representation," *IEEE Transactions on Pattern Analysis and Machine Intelligence*, Vol. 11, No. 7, 1989, pp. 674–693. doi:10.1109/34.192463

[55] Yen, G. G., and Lin, K.-C., "Wavelet Packet Feature Extraction for Vibration Monitoring," *IEEE Transactions on Industrial Electronics*, Vol. 47, No. 3, 2000, pp. 650–667. doi:10.1109/41.847906

[56] Sun, Z., and Chang, C. C., "Structural Damage Assessment Based on Wavelet Packet Transform," *Journal of Structural Engineering*, Vol. 128, No. 10, 2002, pp. 1354–1361. doi:10.1061/(ASCE)0733-9445(2002)128:10(1354)

[57] Karim, A., and Adeli, H., "Incident Detection Algorithm Using Wavelet Energy Representation of Traffic Pattern," *Journal of Transportation Engineering / American Society of Civil Engineers*, Vol. 128, No. 3, 2002, pp. 223–242. doi:10.1061/(ASCE)0733-947X(2002)128:3(232)

[58] Burrus, C. S., Gopinath, R. A., and Guo, H., *Introduction to Wavelets and Wavelet Transforms: a Primer*, Prentice–Hall, Upper Saddle River, NJ, 1998.

[59] Welch, P. D., "The Use of Fast Fourier Transform for the Estimation of Power Spectra: A Method Based on Time Averaging over Short, Modified Periodograms," *IEEE Transactions on Audio and Electroacoustics*, Vol. 15, No. 2, 1967, pp. 70–73. doi:10.1109/TAU.1967.1161901

[60] Babuska, I., and Oden, J. T., "Verification and Validation in Computational Engineering and Science: Basic Concepts," *Computer Methods in Applied Mechanics and Engineering*, Vol. 193, Nos. 36–38, 2004, pp. 4057–4066. doi:10.1016/j.cma.2004.03.002

[61] Oberkampf, W. L., and Barone, M. F., "Measures of Agreement Between Computation and Experiment: Validation Metrics," *Journal of Computational Physics*, Vol. 217, No. 1, 2006, pp. 5–36. doi:10.1016/j.jcp.2006.03.037

[62] Genz, A., "Numerical Computation of Multivariate Normal Probabilities," *Journal of Computational and Graphical Statistics*, Vol. 1, No. 2, 1992, pp. 141–149. doi:10.2307/1390838

[63] Migon, H. S., and Gamerman, D., *Statistical Inference—An Integrated Approach*, Hodder Arnold, London, 1999.

[64] Kass, R., and Raftery, A., "Bayes Factors," *Journal of the American Statistical Association*, Vol. 90, No. 430, 1995, pp. 773–795. doi:10.2307/2291091

[65] Box, G. E. P., and Cox, D. R., "An Analysis of Transformations," *Journal of the Royal Statistical Society Series B (Methodological)*, Vol. 26, No. 2, 1964, pp. 211–52.

[66] Bowman, A. W., and Azzalini, A., *Applied Smoothing Techniques for Data Analysis*, Oxford Univ. Press, New York, 1997.

F. Pai
Associate Editor